Rotor Position Estimation of Switched Reluctance Motors Based on Damped Voltage Resonance

Kristof Geldhof, *Student Member, IEEE,* Alex Van den Bossche, *Senior Member, IEEE* and Jan Melkebeek, *Senior Member, IEEE*

***Index Terms*—Switched Reluctance Motor, Position Estimation, Resonance, Test Pulse**

***Abstract*—This paper proposes a method to obtain the rotor position of switched reluctance motors by means of voltage measurements. It is shown that the combination of motor and power-electronic converter defines a resonant circuit, comprised by the motor phase inductances and the parasitic capacitance of converter switches, power cables and motor phase windings. For salient machines in general, the associated resonance frequency of the circuit depends on the rotor position. In the position estimation method, an initial voltage distribution is imposed over the impedances of the resonance circuit, after which the circuit is let to oscillate freely. During this phase of free oscillation, the induced voltage over a phase winding exhibits a damped oscillatory behaviour, from which position information can be retrieved.**

An overview is given of different possibilities to trigger the voltage resonance. It is shown that the proposed position estimation method has favourable characteristics such as measurement of large-amplitude voltages, robustness against temperature deviations of motor and power semiconductors, very high update rates for the estimated position and absence of sound and disturbance torque. Experimental results are given for a sensorless commutation scheme of a switched reluctance motor under small load.

I. Introduction

POSITION- or speed-sensorless control of electrical machines receives a lot of interest from the industrial and academic community. The advantages of omitting a mechanical position or speed sensor are apparent: a lower cost, a smaller volume and an increased reliability of the drive, especially in environments that feature sensor-agressive conditions, such as dust, moist or mechanical vibrations.

When the aim of a sensorless strategy is to estimate the electrical or mechanical rotor position, some kind of saliency, i.e. a different magnetic behaviour along different geometrical axes, is required. The saliency can have a geometrical origin, for example due to a varying air gap or to the presence of permanent magnets, but it can also be induced by a change of permeability, typically caused by saturation.

One class of position-sensorless strategies measures the slope of phase currents ($\mathrm{d}i/\mathrm{d}t$) to retrieve inductance and position information [1] [2]. The slope of the phase currents can be measured under normal operation or high-frequency distortions can be intentionally superposed on the normal current waveforms [1]. The drawback is that the $\mathrm{d}i/\mathrm{d}t$ is determined by the incremental inductance, which typically decreases at high loads due to saturation or cross-saturation of the magnetic core. This results in a reduced saliency and reduced position estimation accuracy [3]. Alternatively, if normal motor operation allows for periods of zero-current in a phase, voltage test pulses can be applied to this idle phase [4] [5]. This method can give reliable position information, but at the cost of additional torque ripple.

Another class of position-sensorless strategies uses flux estimators, for example by integration of the estimated induced voltage. Provided an online stator resistance estimator (e.g. as described in [6]) is provided, these strategies show good performance at medium to high speeds, but very poor performance at low speeds, due to integration of small errors over a relatively long time [7] [8]. At standstill no position estimation is possible. Direct torque control strategies [9] are also based on flux estimation.

Yet another strategy is based on excitation of motor phases with a high-frequency small-amplitude sinusoidal signal. In one case, a PWM-generated sinusoidal voltage can be superposed on the active phase voltage waveform [10]. This leads to a position-dependent modulation of the phase current. In a second case, external hardware can be used to generate a sinusoidal voltage which is injected into an resonant circuit comprising an idle motor phase and an external capacitor [11] [12]. The inductance or position estimation relies on the measurement of position-modulated currents or voltages. The drawback of these methods is the need for extra hardware to create a sustained oscillation.

There is also a class of methods that uses observers for position or speed tracking. One example of these methods is given by [13]. Generally, a good estimation of motor parameters such as stator resistance and machine-load inertia is required to obtain good tracking behaviour.

This paper presents a position estimation method for salient machines based on the measurement of voltage resonance in an idle phase. The resonance originates from the energy exchange between the inductance and parasitic capacitances of the motor-converter combination. Different methods to trigger the position-dependent resonance are discussed. It is shown that the position information can be retrieved from a large-amplitude signal without generating disturbance torque.

Although the theory is applicable to salient machines which

Manuscript received February 14, 2009. Accepted for publication November 19, 2009.

The authors are with the Department of Electrical Energy, Systems and Automation, Ghent University, Ghent 9000, Belgium (e-mail: kristof.geldhof@ugent.be).

have phases that exhibit periods of zero-current [14], this paper will discuss the method for one class of these machines, namely switched reluctance motors. Experimental results are presented for a 6x4 switched reluctance machine. The position estimation method is described in detail for low-load conditions. Research on how to extend the method for motors under large load is ongoing and is not covered in this paper.

II. Resonant Circuit Model

Fig. 1 shows a configuration comprising an asymmetric H-bridge of a switched reluctance drive converter and a motor phase. This configuration will be used to derive a resonant circuit model, although other types of converters and other devices than IGBTs could be considered.

It is assumed here that the IGBTs and freewheeling diodes are blocked, which means that the behaviour of these devices is mainly determined by a parasitic capacitance. The physical origin of this capacitance lies in the depletion layer, which is essentially an isolating layer between the conducting doped regions of the semiconductor devices. The capacitances C_i and C_d for the IGBTs and diodes respectively are indicated in the parasitic model of Fig. 2. This model also shows the bus bar capacitance C_b, the capacitance C_c of the power cable between H-bridge and motor phase, and the parasitic capacitance C_w of the motor phase winding. The latter is a discrete equivalent for the distributed inter-turn capacitances of the winding. The impedance $\underline{Z}_\mathrm{w}$ represents the phase winding impedance without the contribution of the parasitic capacitance C_w.

In the frequency domain, the impedance $\underline{Z}_\mathrm{w}$ depends not only on the rotor position θ, but on the frequency ω as well, due to induced eddy currents and hysteresis in the magnetic circuit. The impedance $\underline{Z}_\mathrm{w}$ can be measured [15] or it can be obtained by means of a static finite element calculation, in which the permeability μ of the magnetic core is replaced by a complex permeability $\underline{\mu}_c$ [16] [17], given by:

$$s\underline{\mu}_c(s) = \frac{2}{d}\sqrt{\frac{s\mu}{\sigma}}\tanh\left(\sqrt{s\mu\sigma}\frac{d}{2}\right). \tag{1}$$

In (1), s stands for the laplace operator, d is the thickness of a magnetic sheet in the laminated core and σ is the specific conductivity of the core material. For a given frequency ω, the wide-frequency permeability model (1) can be evaluated in $s = j\omega$, and the resulting phase impedance $\underline{Z}_\mathrm{w}(\theta, j\omega)$ can be calculated. The real and imaginary part of the admittance $\underline{Y}_\mathrm{w} = 1/\underline{Z}_\mathrm{w}$ can be associated with an inductance L_w and an eddy current loss resistance R_w respectively, as indicated in Fig. 2.

The permeability model (1) can be modified to take into account hysteresis losses as well [16] [17]. The model has been experimentally validated on a 6x4 switched reluctance motor [18]. It was concluded that an increasing frequency leads to a decrease in phase winding inductance and an increase in the losses. The inductance decrease is most pronounced when the rotor is in the aligned position in respect to the excited stator phase.

We will assume here that the parasitic capacitances C_i and C_d of the semiconductor devices are constant. This is a strong simplification, as both capacitances show a strong nonlinear dependence on the voltage across them. With the constant capacitance assumption, the combined motor-converter circuit reduces to the equivalent parallel LRC circuit of Fig. 3, with an equivalent capacitance C_eq given by

$$C_\mathrm{eq} = \frac{C_\mathrm{i} + C_\mathrm{d}}{2} + C_\mathrm{c} + C_\mathrm{w}. \tag{2}$$

In the derivation of the equivalent circuit capacitance C_eq we have assumed that the bus bar capacitance C_b is at least a factor 100 larger than the parasitic capacitances C_i and C_d. This is a realistic assumption: the bus bar capacitor is typically quite large as it has the function of an energy buffer, in order to limit bus bar voltage fluctuations. If the frequency is large enough, the bus bar impedance $\underline{Z}_\mathrm{b} = 1/(j\omega C_\mathrm{b})$ is approximately a short-circuit and therefore decouples the different phases at the converter side.

The circuit of Fig. 3 has an undamped resonance frequency ω_res given by

$$\omega_\mathrm{res} = \frac{1}{\sqrt{L_\mathrm{w}(\theta, \omega_\mathrm{res})C_\mathrm{eq}}} \tag{3}$$

As can be seen from (3), ω_res depends on the rotor position. The undamped resonance frequency will reach a maximum value for the unaligned rotor position and a minimum value for the aligned rotor position.

III. Resonance Triggers

In the previous section, it was discussed that the motor-converter system defines a circuit which has a position-

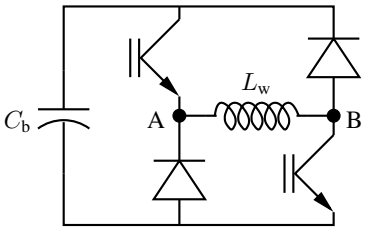

Fig. 1. Converter H-bridge and phase winding

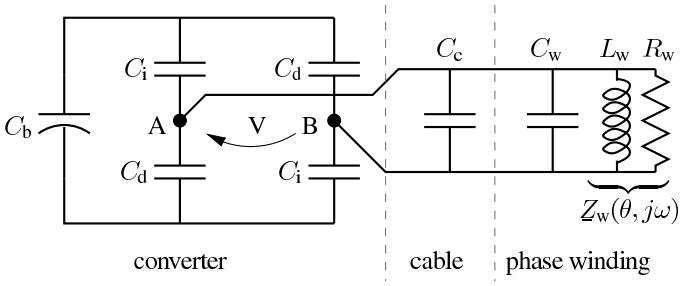

Fig. 2. Parasitic model of motor-converter combination

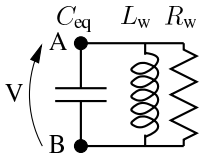

Fig. 3. Equivalent resonant LRC circuit

dependent resonance frequency. In order to observe a resonance, an initial voltage and/or current distribution has to be realized, after which the circuit is let to oscillate freely, thereby exchanging energy between its capacitive and inductive elements. The process of setting these initial conditions in the resonant circuit will be defined as a *resonance trigger*.

There are several ways by which a resonance can be triggered in the motor-converter system. All of them have in common that an initial voltage and/or current distribution is defined in the elements of Fig. 2, after which the system is let to oscillate freely.

The following sections describe the different resonance triggers by means of experimental results. All measurements were done on a 6x4 switched reluctance motor with rated torque 19.3 Nm and base speed 2140 rpm. The minimum and maximum static phase inductance are 13 mH and 80 mH respectively. The motor phase windings were connected to an asymmetrical H-bridge converter, comprised by Fairchild FCAS50SN60 smart power modules. The IGBTs in the power modules were controlled by the PWM generators of a Freescale MC56F8367 DSP evaluation board.

A. Resonance after Diode Recovery

If both IGBTs are switched off in a conducting motor phase, the phase current commutates to the freewheeling diodes and decreases. The current will become zero and will even change its sign, until recovery of the diodes takes place. After recovery, the phase voltage exhibits a strongly damped oscillating behaviour as can be seen in Fig. 4(b) for both unaligned and aligned rotor position.

The initial conditions for the resonance are set at the end of diode recovery, when each diode starts to behave as a parasitic capacitance C_d; the corresponding voltage distribution is shown in Fig. 5. Initial electrostatic energy is present in the parasitic capacitance of each IGBT ($E_\mathrm{i} = \frac{1}{2}C_\mathrm{i}V_\mathrm{dc}^2$) and in the parasitic capacitance of cable and phase winding ($E_\mathrm{c}+E_\mathrm{w} = \frac{1}{2}(C_\mathrm{c}+C_\mathrm{w})V_\mathrm{dc}^2$). The small forward voltage drop over the diodes at the end of recovery is neglected here. Also, an initial magnetostatic energy is stored in the phase inductor ($E_\mathrm{l} = \frac{1}{2}L_\mathrm{w}I_\mathrm{RRC}^2$), where I_RRC is the reverse recovery current of the diodes.

The exchange of energy between the capacitive and inductive elements results in a resonance, which can clearly be observed in the phase voltage (see Fig. 4(b)), as well as in the phase current (but on a much smaller scale, see the magnification in Fig. 4(c)). The resonances are damped due to eddy current and hysteresis loss in the magnetic core of the machine. The damping is stronger in the aligned rotor position, as the peak induction in the magnetic material is higher compared to the unaligned rotor position.

The difference in resonance between the aligned and unaligned rotor position can be used to obtain position information. In a very simple implementation, diagnostic pulses could be applied to an idle motor phase. One sample of the resonating phase voltage could be measured at a fixed time δ after the switch-on command for the IGBTs, as indicated in Fig. 4(b). By means of an (initially established) mapping

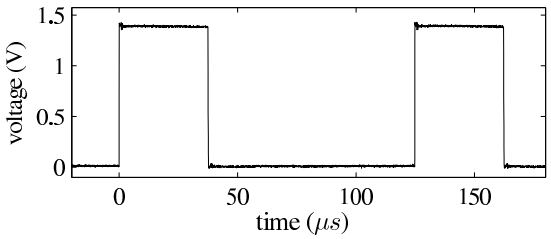

(a) Control signal for IGBTs (signal before gate drive circuit).

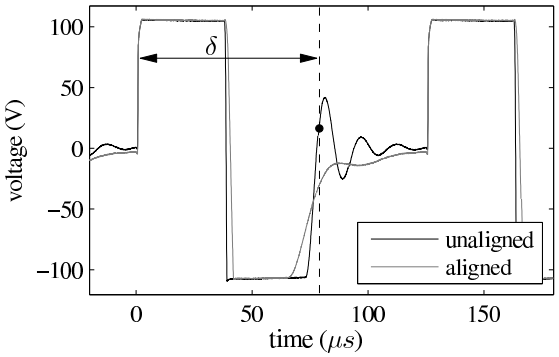

(b) Phase voltage. The time delay between the switch-on command for the IGBTs and the measurement of one sample on the voltage resonance is indicated by δ.

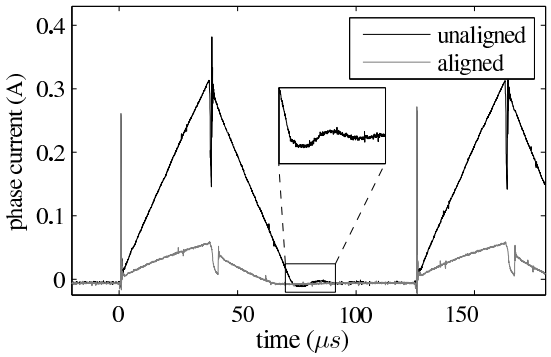

(c) Phase currents and magnification of current resonance for the unaligned rotor position.

Fig. 4. Measured resonance after diode recovery for the unaligned and aligned rotor position. A bus bar voltage V_dc=105 V was used and diagnostic voltage pulses were applied at a rate of 8 kHz and with 30 % duty ratio.

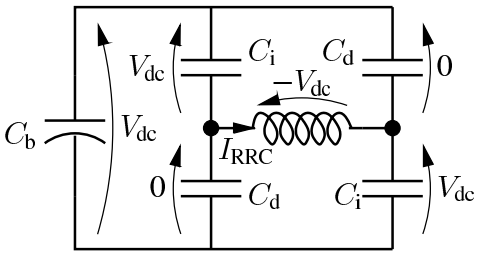

Fig. 5. Initial energy distribution at diode recovery

between the measured voltage and the rotor position, the position could be retrieved.

However, there are some important disturbance factors when using the recovery-triggered resonance for position estimation:

- The recovery time of the diodes depends on the phase current $\mathrm{d}i/\mathrm{d}t$ prior to recovery [19] [20]. The large saliency ratio of a switched reluctance motor corresponds to a large difference in $\mathrm{d}i/\mathrm{d}t$ between the unaligned and aligned rotor position, see Fig. 4(c). It can be seen from Fig. 4(b) that the unaligned resonance starts about 10 μs after the start of the aligned resonance. This results in an intersection between both resonances. In a worst-case situation, the voltage sample is taken at the intersection, and it cannot be distinguished between unaligned or aligned position. Taking the sample before or after the intersection leads to a decreased voltage (and thus position) resolution compared to the (ideal) case where recovery would not depend on the position.
- The recovery time depends on the diode junction temperature [19] [20], and thus on the load of the machine.

B. Resonance after IGBT switch-off

A closer look at Fig. 4(b) reveals that the $\mathrm{d}v/\mathrm{d}t$ of the phase voltage after switch-off of both IGBTs (at $t \approx 42$ μs) differs between the unaligned and aligned rotor position. The waveform of the phase voltage as it evolves from $+V_{\mathrm{dc}}$ to $-V_{\mathrm{dc}}$ is actually a resonance on its own, defined by the same parasitic capacitances and phase inductance as discussed in section III-A. The difference is that, at the time of IGBT switch-off, a significant amount of magnetic energy $\frac{1}{2}L_{\mathrm{w}}I^2$ is stored in the phase inductance L_{w} compared to the energy $E_{\mathrm{l}} = \frac{1}{2}L_{\mathrm{w}}I^2_{\mathrm{RRC}}$ at diode recovery. For the undamped LC ciruit of Fig. 6, the influence of the initial magnetically stored energy on the voltage resonance is illustrated in Fig. 7.

Suppose that this circuit has following initial conditions:

$$v(t=0) = V_0, \tag{4}$$
$$i(t=0) = I_0. \tag{5}$$

The voltage waveform that satisfies these initial conditions is

$$v(t) = -\sqrt{\frac{L}{C}} I_0 \sin(\omega_{\mathrm{res}} t) + V_0 \cos(\omega_{\mathrm{res}} t), \tag{6}$$

with

$$\omega_{\mathrm{res}} = \frac{1}{\sqrt{LC}}. \tag{7}$$

The characteristic impedance

$$Z_0 = \sqrt{\frac{L}{C}} \tag{8}$$

is typically in the order of $k\Omega$. It can thus be seen that, for normal operating currents, the resonance will be mainly determined by the first term in (6). Due to the initial current I_0 in the inductor, the resonating voltage waveform will overshoot the $-V_0$ voltage level, see Fig. 7. For the motor-converter combination, this means that the freewheeling diodes take over as soon as this voltage level is trespassed, see Fig. 4(b).

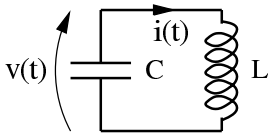

Fig. 6. Undamped LC circuit

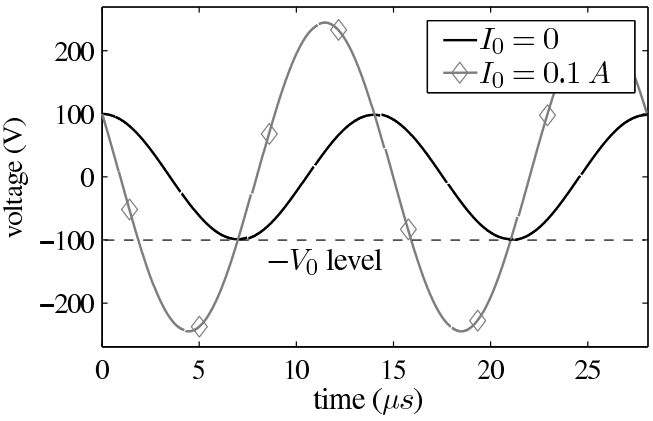

Fig. 7. Simulated response of the undamped LC circuit of Fig. 6 (with $L = 5$ mH, $C = 1$ nF) for an initial current $I_0 = 0$ and for an initial current $I_0 = 0.1\ A$. In both cases, the initial voltage V_0 is 100 V.

The advantage of using the voltage resonance after IGBT switch-off is that the switching actions under normal motor operation could be used to detect the rotor position. However, one has to take into account that:

- an extree degree of freedom, namely the phase current, is involved in the mapping of the resonance waveform to a rotor position,
- the current has to be known accurately at the moment of IGBT switch-off. A small error in the measured current leads to a significant deviation of the estimated rotor position. The need for an accurate current measurement at the moment of switch-off increases the hardware and software complexity, as most drives sample the phase current only half-way of two switching instants in a PWM period.

C. Resonance Triggering by Short Voltage Pulses

In the previous section, the influence of the phase current on the voltage resonance was discussed. A logical conclusion would be to use an idle phase and reduce the amount of on-time of the IGBTs in order to limit the build-up of current (and magnetic energy) in the phase winding inductance [14]. Fig. 8 shows measurements of the phase voltage for decreasing on-times of the IGBTs. If the IGBTs are switched on for only a very short time (about 1.8 μs or smaller), the magnetic energy stored in the inductor becomes so small that the voltage resonance shows no overshoot at all, so that the freewheeling diodes do not conduct. The voltage shows a damped oscillation until all initially stored energy has been dissipated.

Figure. 8 also shows that, if the IGBT on-time is further reduced below 1.2 μs, the IGBTs are not fully switched on anymore, which results in an increased voltage drop over the IGBTs and a reduced initial phase voltage.

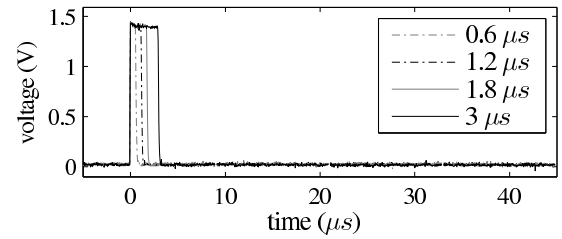

(a) Control signal for IGBTs (signal before gate drive circuit)

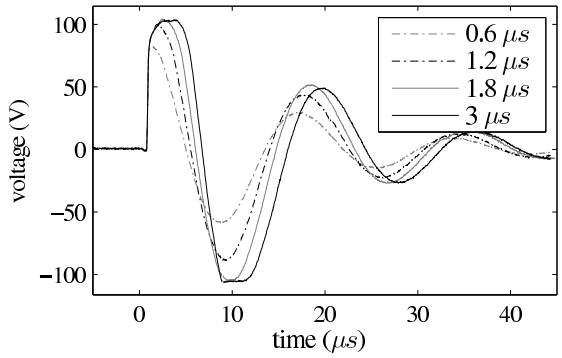

(b) Phase voltage

Fig. 8. Measured phase voltage response in the unaligned rotor position for different IGBT on-times. DC bus bar voltage $V_{\text{dc}} = 105\ V$.

A position estimation method based on resonance triggering by means of short voltage pulses has several advantages:

- The measured signal has the same order of magnitude of the DC bus bar voltage. From Fig. 8(b) it can be seen that the first part of the resonance triggered by a 1.8 μs pulse varies between approximately +100 V and -100 V. Such a large-amplitude signal is less prone to disturbances compared to signals of small amplitude.
- The resonance starts almost immediately after the application of a voltage pulse. Position information can therefore be retrieved within microseconds. This allows for very fast updates of the position estimation, even up to 100 kHz.
- During the resonance, the phase current exhibits the same resonance as the phase voltage, but with a very small amplitude, due to the large characteristic impedance (8) of the phase winding. From the magnification of the unaligned phase current response in Fig. 4(c) it can be seen that the peak current during the recovery-triggered resonance is in the order of mA. In the case of resonance triggered by short voltage pulses the current is even smaller. The disturbance torque generated by these currents is therefore negligable.
- Due to the very small currents associated with the resonance, no additional sound is produced.
- The resonance does not vary with junction temperature, as no diode recovery is involved.
- The resonance does not vary with motor temperature. The specific conductivity σ of electrical steel (which determines the eddy-current-induced damping of the resonance) is practically constant over a wide range of operating temperatures.

It is important to note that *both* IGBTs have to be switched on and off simultaneously. This ensures that the potential of point A in Fig. 2 is pulled up to the positive bus bar potential and that the potential of point B is pulled down to the negative bus bar potential. The initial phase voltage equals the bus bar voltage V_{dc} in this case.

If only the upper IGBT in the H-bridge is switched on, this would leave the potential of point B undefined, i.e. depending on secondary parasitic effects such as leakage currents of the power semiconductor devices and parasitic capacitances to earth or other parts of the circuit. The initial phase voltage would then not necessarily be equal to the bus bar voltage V_{dc}, resulting in a resonance with unpredictable amplitude.

IV. Rotor Position Mapping

In the previous section it has been shown that, by means of applying short voltage pulses, a position-dependent voltage resonance can be triggered. There are several possibilities to extract rotor position information from the damped resonance. Probably the most simple method involves a single measurement of the resonating voltage, at a fixed time after the application of the voltage pulse.

Fig. 9(b) shows an experimental result at standstill of phase voltage resonances triggered by a 1.2 μs pulse, for the unaligned and aligned rotor position of phase C respectively. The voltage test pulse is applied in phase C, while PWM current control is applied in the active phase A, as can be seen from Fig. 9(a). Due to capacitive and inductive coupling between both phases, the switching actions in phase A induce a voltage in the idle phase C, as indicated by the arrows in Fig. 9(b). If a switching action occurs in the active phase at a time instant close to the measurement of the voltage resonance, the induced voltage would disturb the resonance, resulting in a position estimation error. In order to prevent this situation, the timing of the test pulse is synchronized with the pulse width modulation in the active phase, in such a way that the part of the voltage resonance before the sampling instant lies in a period in which no switching actions occur.

If the resonances are measured at a fixed time t_s [1] relative to the start of each pulse, each voltage sample can be mapped to the rotor position at which the sample was measured. As a consequence, the measured voltage samples form a position signature of the combination of motor (phase C) and converter. Fig. 10 shows this signature, for the chosen sample time t_s as indicated in Fig. 9(c). This signature was obtained by manually rotating the SRM over 90° mechanical. At successive steps of 1°, the voltage at time t_s was obtained with the cursor function of an oscilloscope on which the resonance was visualized.

V. Sensorless commutation

For applications that do not require high dynamics, it is sufficient to determine the appropriate rotor angles for phase

[1] If the sample time t_s is chosen close before the most negative voltage in the unaligned resonance, the difference between the unaligned and aligned voltage values at t_s is large, and a good position resolution is achieved.

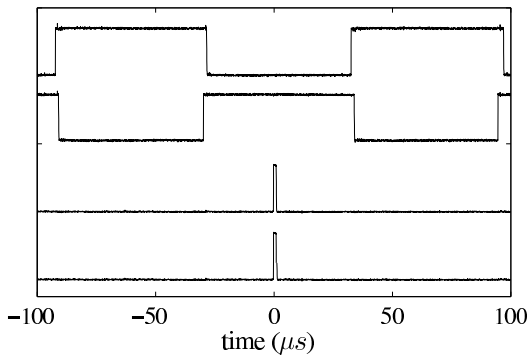

(a) Control signal for IGBTs of the active phase A (top waveforms) and the idle phase C (bottom waveforms). The current in the active phase is controlled at 2.5 A by an 8 kHz PWM current control.

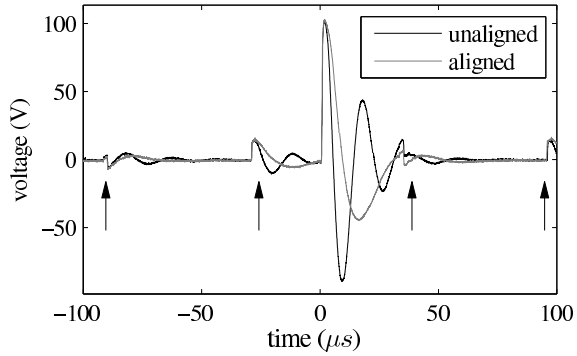

(b) Phase voltage resonance. Arrows indicate induced voltages triggered by switching actions in the active phase.

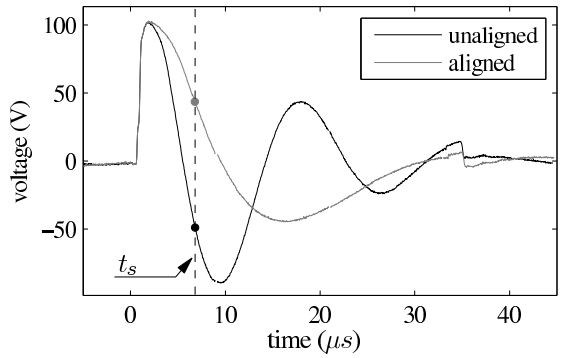

(c) Detail of (b). The resonance is sampled at time t_s.

Fig. 9. Measured resonance after application of a 1.2 μs voltage pulse in phase C, for the unaligned and aligned position with respect to phase C. Phase A is current-controlled. DC bus bar voltage $V_{\rm dc} = 105\ V$.

commutation. This section describes a possible implementation for sensorless commutation by means of measuring voltage resonance.

Suppose that for a given rotation direction, the motor must commutate according to the phase sequence C→B→A→C→... . If phase A is the active phase, voltage resonance can be triggered in the leading phase C, which is idle. The rotor angle at which phase A should commutate to phase C corresponds with a voltage in the position signature of phase C. In the SRM of the experimental setup, the active

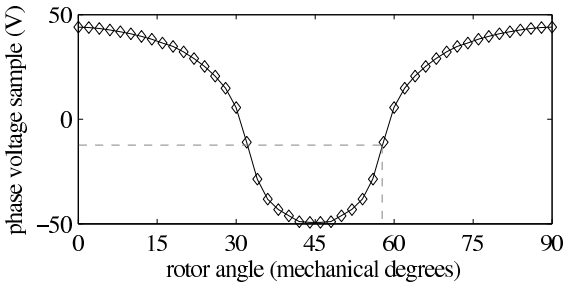

Fig. 10. Measured phase C position signature for the 6x4 switched reluctance motor. The aligned rotor position corresponds to 0°, the unaligned position corresponds to 45°. The point (56°,-10 V) defines the angle/voltage for the active phase commutation A→C.

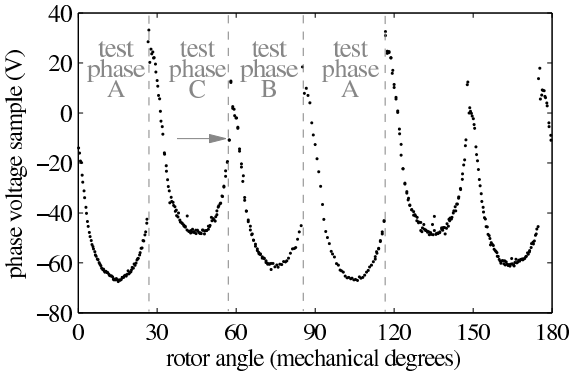

Fig. 11. Measured voltage samples during sensorless operation. The SRM is operated in current-control mode at 2.5 A. Speed≈120 rpm. DC bus bar voltage $V_{\rm dc} = 105\ V$. The aligned position of phase C corresponds to 0°, the unaligned position corresponds to 45°. The arrow indicates the -10 V treshold for active phase commutation A→C.

phase commutation A→C should occur at a rotor angle of 56°. Inspection of Fig. 10 shows that the corresponding voltage treshold is -10 V. Therefore, the commutation command is issued if the voltage resonance sample crosses this threshold with a positive edge (the condition of a positive edge is required to exclude the 34° angle, which also corresponds with the -10 V treshold).

Fig. 11 shows measurements of the resonance voltage in the subsequent idle phases as a function of rotor position during sensorless operation of the SRM. The SRM is slightly loaded by the friction torque of a permanent-magnet motor, the shaft of which is coupled with the shaft of the SRM. The SRM is operated in current-control mode with set point 2.5 A, resulting in a speed of approximately 120 rpm. During the application of test pulses in consecutive phases of the machine (at 30° intervals), a part of the position signature associated with each phase can be observed. For test phase C, the voltage samples in the position interval [26°,56°] correspond to the samples of Fig. 10 in the same angular range.

From Fig. 11 it is clear that the position signatures for the three phases are not identical. Possible reasons for this fact are geometrical motor asymmetry (for example an egg-shaped stator) or different gain factors in the voltage measurement and analog-to-digital conversion circuit. It is therefore preferable to define three different commutation voltages associated to

the respective phases, as has been done in the experiment.

As can be seen from Fig. 10, the position signature has a high sensitivity with respect to the rotor position in the region around the commutation angle (56°). The commutation error remains smaller than 1° for all phases in a speed range between standstill and approximately 50% of the rated speed (N_{rated}=2140 rpm) of the SRM. At higher speeds, the induced EMF in the idle phase influences the position estimation. This effect can be compensated for, so that a larger speed range can be obtained. However, this is not further discussed in this paper.

The experimental results given in this section are valid for a machine under light load, which implies that no saturation of the magnetic paths occurs. The influence of saturation and cross-saturation between phases will be discussed in a future paper.

VI. Conclusions

This paper proposed a position estimation method for switched reluctance motors, based on voltage resonance. The combination of a phase winding with the power-electronic converter defines a resonant circuit, comprising the motor phase inductance and parasitic capacitances of phase winding, power-electronic switches and power cable. The associated resonance frequency depends on the rotor position. Three methods of resonance triggering have been discussed: triggering by diode recovery, resonance triggering after IGBT switch-off and triggering by applying short voltage pulses. By means of measuring the resonance of the induced phase voltage, the rotor position can be retrieved within one electrical cycle of the motor. Experimental results were presented for a sensorless commutation scheme of a 6x4 switched reluctance motor under small load.

It has been shown that the proposed position estimation method has favourable characteristics such as: measurement of large-amplitude voltages, robustness against temperature deviations of motor and power semiconductors, very high update rates for the estimated position and absence of disturbance torque.

References

[1] F. M. L. De Belie, P. Sergeant, and J. A. A. Melkebeek, "Reducing steady-state current distortions in sensorless control strategies by using adaptive test pulses," *Twenty-Third Annual IEEE Applied Power Electronics Conference and Exposition, APEC 2008*, pp. 121–126, Feb. 2008.

[2] P. P. Acarnley, R. J. Hill, and C. W. Hooper, "Detection of rotor position in stepping and switched motors by monitoring of current waveforms," *IEEE Trans. Ind. Electron.*, vol. 32, no. 3, pp. 215–222, Aug. 1985.

[3] P. Sergeant, F. M. L. De Belie, and J. A. A. Melkebeek, "Effect of rotor geometry and magnetic saturation in sensorless control of PM synchronous machines," *IEEE Trans. Magn.*, vol. 45, no. 3, Mar. 2009.

[4] W. D. Harris and J. H. Lang, "A simple motion estimator for variable-reluctance motors," *IEEE Trans. Ind. Appl.*, vol. 26, no. 2, pp. 237–243, Mar./Apr. 1990.

[5] K. R. Geldhof, A. Van den Bossche, T. J. Vyncke, and J. A. A. Melkebeek, "Influence of flux penetration on inductance and rotor position estimation accuracy of switched reluctance machines," in *34th Annual Conference of IEEE Industrial Electronics, IECON 2008*, Orlando, USA, Nov. 10–13, 2008, pp. 1246–1251.

[6] N. H. Fuengwarodsakul, S. E. Bauer, J. Krane, C. P. Dick, and R. W. De Doncker, "Sensorless direct instantaneous torque control for switched reluctance machines," in *European Conference on Power Electronics and Applications.*, Dresden, Germany, Sep. 11–14, 2005, paper 385.

[7] D. Panda and V. Ramanarayanan, "Reduced acoustic noise variable DC-bus-voltage-based sensorless switched reluctance motor drive for HVAC applications," *IEEE Trans. Ind. Electron.*, vol. 54, no. 4, pp. 2065–2078, Aug. 2007.

[8] I. Al-Bahadly, "Examination of a sensorless rotor-position-measurement method for switched reluctance drive," *IEEE Trans. Ind. Electron.*, vol. 55, no. 1, pp. 288–295, Jan. 2008.

[9] R. B. Inderka and R. W. A. A. De Doncker, "DITC-direct instantaneous torque control of switched reluctance drives," *IEEE Trans. Ind. Appl.*, vol. 39, no. 4, pp. 1046–1051, Jul./Aug. 2003.

[10] H. Kim, M. C. Harke, and R. D. Lorenz, "Sensorless control of interior permanent-magnet machine drives with zero-phase lag position estimation," *IEEE Trans. Ind. Appl.*, vol. 39, pp. 1726–1733, Nov./Dec. 2003.

[11] P. Laurent, M. Gabsi, and B. Multon, "Sensorless rotor position analysis using resonant method for switched reluctance motor," in *Conference Record of the 1993 IEEE Industry Applications Society Annual Meeting*, vol. 1, Toronto, Canada, Oct. 1993, pp. 687–694.

[12] J. R. Goetz, K. J. Stalsberg, and W. A. Harris, "Switched reluctance motor position by resonant signal injection," European Patent Application EP19 960 102 892, Feb. 17, 1992.

[13] A. Lumsdaine and J. Lang, "State observers for variable-reluctance motors," *IEEE Trans. Ind. Electron.*, vol. 37, no. 2, pp. 133–142, Apr. 1990.

[14] K. Geldhof and A. Van den Bossche, "Resonance-based rotor position estimation in salient machines," European Patent Request PCT/EP2009/057 125, Jun. 10, 2009 (prio filing GB0813226.8 - Jul. 18, 2008).

[15] J. Corda and S. M. Jamil, "Experimental determination of equivalent circuit parameters of a tubular switched reluctance machine with solid steel magnetic core," *IEEE Trans. Ind. Electron.*, vol. 56, no. 12, 2009, to be published.

[16] A. Van den Bossche, V. C. Valchev, and M. De Wulf, "Wide frequency complex permeability function for linear magnetic materials," *Journal of Magnetism and Magnetic Materials*, vol. 272-276, no. 1, pp. 743–744, May 2004.

[17] A. Van den Bossche and V. C. Valchev, *Inductors and Transformers for Power Electronics*. Boca Raton, USA: CRC press, 2005, ch. 3.

[18] K. R. Geldhof, A. Van den Bossche, and J. A. A. Melkebeek, "Influence of eddy currents on resonance-based position estimation of switched reluctance drives," in *International Conference on Electrical Machines and Systems, ICEMS 2008*, Wuhan, China, Oct. 17–20, 2008, pp. 2820–2825.

[19] A. Emadi, Ed., *Handbook of automotive power electronics and motor drives*. CRC-press, 2005, ch. 6.

[20] P. Haaf and J. Harper. Understanding diode reverse recovery and its effect on switching losses. Fairchild On-Demand Webinar. [Online]. Available: http://www.techonline.com/learning/webinar/202802635

Kristof R. Geldhof (S'04) received the M.S. degree in electromechanical engineering from Ghent University Belgium, in 2001. Since 2004 he has been with the Electrical Energy Laboratory (EELAB), Department of Electrical Energy, Systems and Automation (EESA) of Ghent University. He is currently working towards a Ph.D. degree. His research focusses on high-dynamic position-sensorless control strategies for switched reluctance motor drives.

Alex P. M. Van den Bossche (M'99–SM'03) received the M.S. and the Ph.D. degrees in electromechanical engineering from Ghent University Belgium, in 1980 and 1990 respectively. He has worked there at the Electrical Energy Laboratory. Since 1993, he is a full professor at the same university in the same field. His research is in the field of electrical drives, power electronics on various converter types and passive components and magnetic materials. He is also interested in renewable energy conversion. He is a senior member of IEEE. He is co-author of the book Inductors and Transformers for Power Electronics.

Jan A. Melkebeek (M'80–SM'85) received the M.S. and the Ph.D. degrees in electromechanical engineering from Ghent University Belgium, in 1975 and 1980 respectively. In 1986 he obtained the degree of 'Doctor Habilitus' in Electrical and Electronical Power Technology, also from Ghent University. Since 1987 he is Professor in Electrical Engineering (Electrical Machines and Power Electronics) at the Engineering Faculty of Ghent University. He is the head of the Department of Electrical Energy, Systems and Automation and the director of the Electrical Energy Laboratory (EELAB). His teaching activities and research interests include electrical machines, power electronics, variable frequency drives, and also control systems theory applied to electrical drives. Prof.dr.ir. J. Melkebeek is a fellow of the IET and a senior member of the IEEE.